Benzyl viologen-assisted simultaneous exfoliation and *n*-doping of MoS_2 nanosheets via a solution process

Kiyoung Jo[†], *Jaeyoo choi*[†], *and Heesuk Kim*[†, ‡, *]

[†]Photo-electronic Hybrids Research Center, Korea Institute of Science and Technology (KIST), Seoul 02792, Republic of Korea. [‡] Nano-Materials and Engineering, Korea University of Science and Technology (UST), Daejeon 34113, Republic of Korea.

KEYWORDS : MoS_2 nanosheets, benzyl viologen, simultaneous exfoliation and *n*-doping, electrical properties, Seebeck coefficient

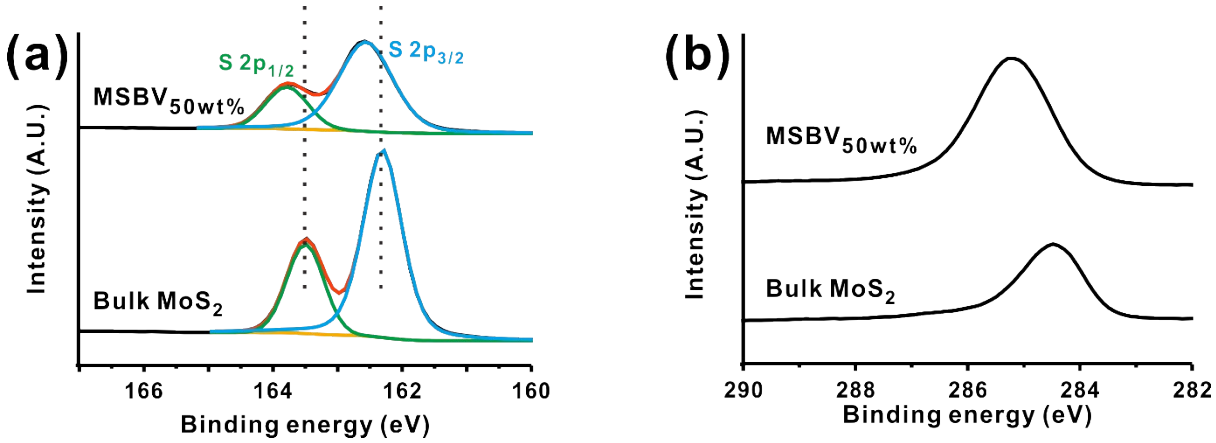

Fig. S1 XPS spectra of (a) S(2p) and (b) C(1s) peaks of bulk MoS_2 and $MSBV_{50wt\%}$.

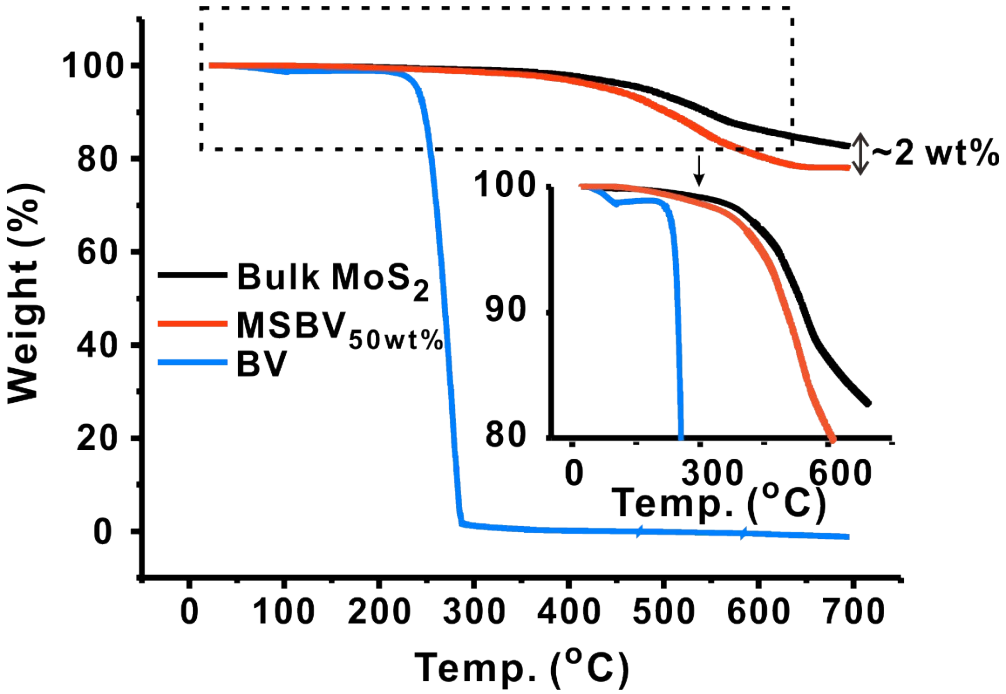

Fig. S2 Thermogravimetric analysis (TGA) data of bulk MoS_2, $BVCl_2$, and $MSBV_{50wt\%}$.

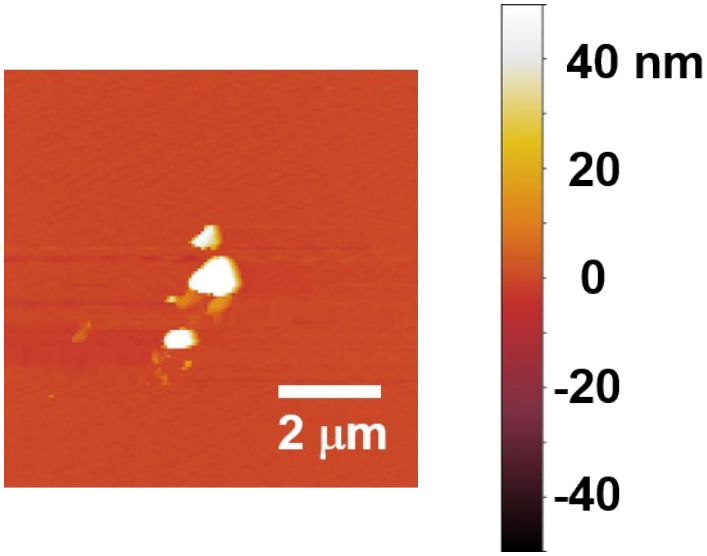

Fig. S3 AFM image of $MSBV_{0wt\%}$ which denotes MoS_2 reacted only with hydrazine.

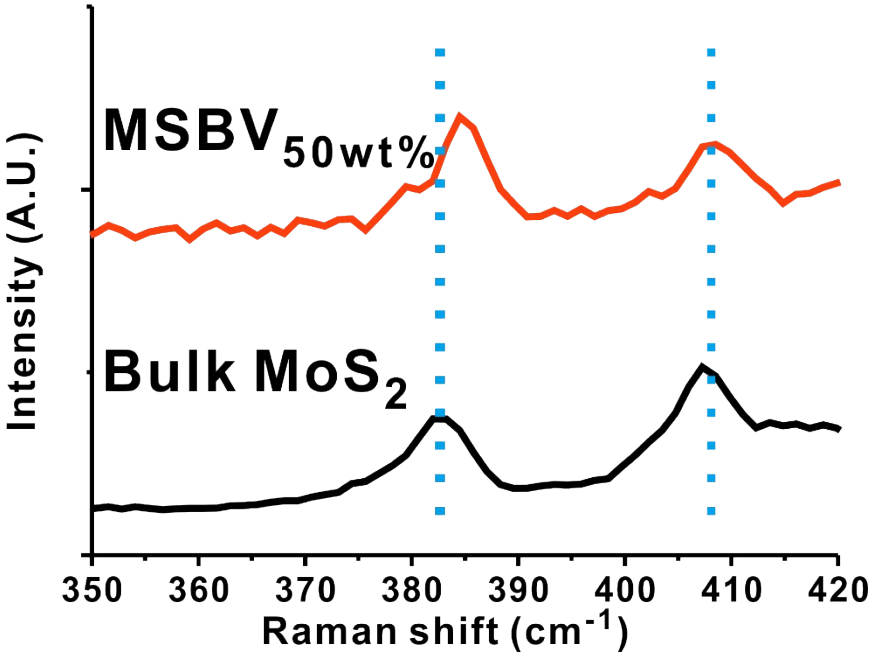

Fig. S4 Raman spectrum of bulk MoS_2 and $MSBV_{50wt\%}$.

The peak separation between A_{1g} and E^1_{2g} mode is dependent on the number of layers.[1] As shown in Figure S4, bulk MoS_2 has its A_{1g} and E^1_{2g} modes at 407.7 and 382.5 cm^{-1}, respectively, leading to a peak separation of 25.2 cm^{-1}. In contrast, the E^1_{2g} mode of $MSBV_{50wt\%}$ upshifts from 382.5 to 385.0 cm^{-1}, creating a peak separation of 22.7 cm^{-1}.

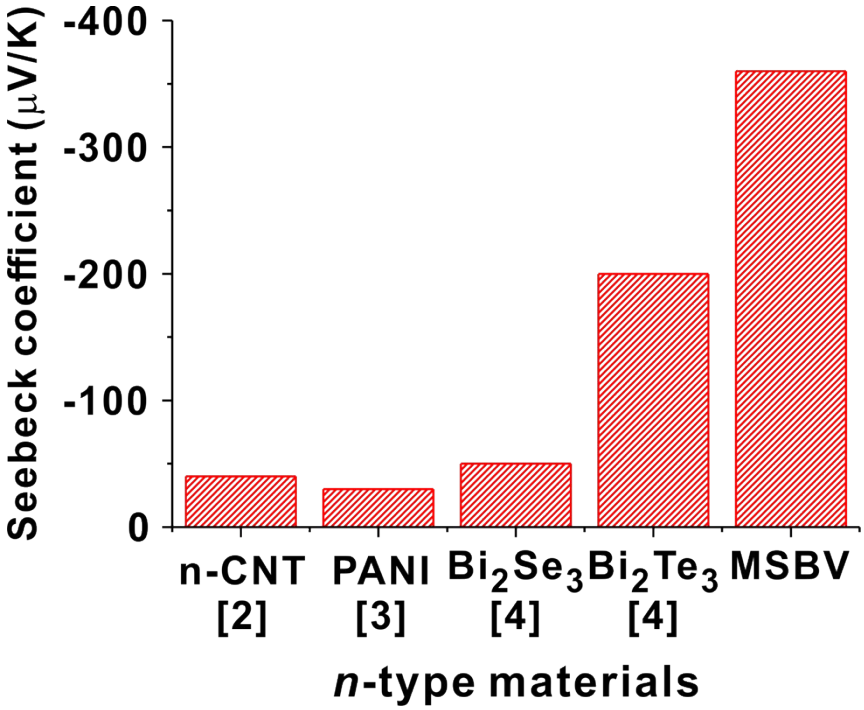

Fig. S5 Seebeck coefficient of $MSBV_{50wt\%}$ and conventional n-type thermoelectric materials at room temperature.

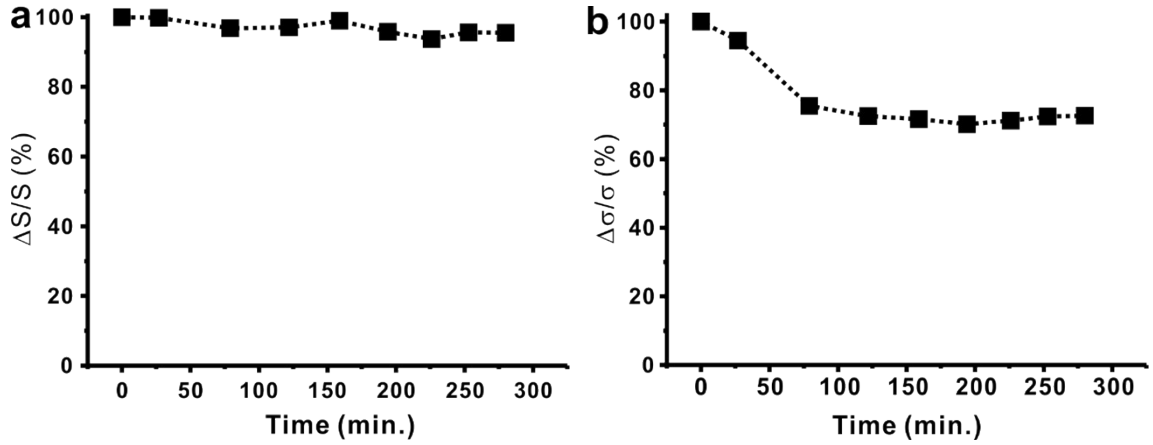

Fig. S6 (a) Seebeck coefficient and (b) electrical conductivity of MSBV50wt% as a function of time.

Table S1. Energy shift of XPS core levels in $MSBV_{50wt\%}$ before and after BV doping.

Peaks	Binding energy (eV)		Binding energy shift (eV)
	Before BV doping	After BV doping	
Mo $3d_{5/2}$	229.48	229.71	+0.23
Mo $3d_{3/2}$	232.63	232.85	+0.22
S $2p_{3/2}$	162.30	162.56	+0.26
S $2p_{1/2}$	163.50	163.79	+0.29

Table S2. Carrier properties of the bulk MoS_2, $MSBV_{0wt\%,}$ $MSBV_{50wt\%}$, and previous *n*-doped MoS_2 monolayers.

	Hall mobility ($cm^2 \cdot V^{-1} \cdot s^{-1}$)	Bulk carrier concentration (cm^{-3})	Sheet carrier concentration (cm^{-2})
Bulk MoS_2	1.40	8.77×10^{13}	9.21×10^{11}
$MSBV_{0wt\%}$	2.30	2.77×10^{13}	2.63×10^{11}
$MSBV_{50wt\%}$	2.39	2.97×10^{14}	2.52×10^{12}
Cl-MoS_2 1L [5]	60.0	N.A.	9.2×10^{12}
Cs_2CO_3-MoS_2 1L [6]	4	N.A.	3.5×10^{11}
BV-MoS_2 1L [7]	24.7	N.A.	1.2×10^{13}
APTMS-MoS_2 1L [8]	2.06	N.A.	7.2×10^{12}

Table S3. S/Mo and O/Mo area ratios of the bulk MoS_2, $MSBV_{50wt\%}$, and $MSBV_{50wt\%}$ annealed at 280 °C. Note that they were calculated by measuring the ratios of the peak areas and correcting them for sensitivity factors to obtain corrected peak area ratios.

	S/Mo	O/Mo (total)	O/Mo (MoO_3)	O/Mo (MoO_2)
Bulk MoS_2	1.90	0.0907	0.0707	0.0200
MSBV	2.01	0.0874	0.0647	0.0227
Annealed MSBV	1.20	0.733	0.613	0.120

References

(1) C. Lee, H. Yan, L. E. Brus, T. F. Heinz, J. Hone and S. Ryu, *ACS Nano*, 2010, **4,** 2695-2700.

(2) T. Fukumaru, T. Fujigaya and N. Nakashima, *Sci. rep.*, 2015, **5,** 7951.

(3) N. Mateeva, H. Niculescu, J. Schlenoff and L. R. Testardi, *J. Appl. Phys.*, 1998, **83,** 3111-3117.

(4) Y. Min, J. W. Roh, H. Yang, M. Park, S. I. Kim, S. Hwang, S. M. Lee, K. H. Lee and U. Jeong, *Adv. Mater.*, 2013, **25,** 1425-1429.

(5) L. Yang, K. Majumdar, H. Liu, Y. Du, H. Wu, M. Hatzistergos, P. Y. Hung, R. Tieckelmann, W. Tsai, C. Hobbs and P. D. Ye, *Nano Lett.*, 2014, **14,** 6275-6280.

(6) J. D. Lin, C. Han, F. Wang, R. Wang, D. Xiang, S. Qin, X.-A. Zhang, L. Wang, H. Zhang, A. T. S. Wee and W. Chen, *ACS Nano*, 2014, **8,** 5323-5329.

(7) D. Kiriya, M. Tosun, P. Zhao, J. S. Kang and A. Javey, *J. Am. Chem. Soc.*, 2014, **136,** 7853-7856.

(8) Y. Li, C.-Y. Xu, P. Hu and L. Zhen, *ACS Nano*, 2013, **7,** 7795-7804.